

1 Microscopic evidence of the connection between liquid-liquid transition and
2 dynamical crossover in an ultra-viscous metallic glass former

3
4 S. Hechler^{1,2}, B. Ruta^{2,3*}, M. Stolpe¹, E. Pineda⁴, Z. Evenson⁵, O. Gross¹, A. Bernasconi^{2,6}, R.
5 Busch¹ and I. Gallino¹

6 ¹ *Chair of Metallic Materials, Department of Materials Science and Engineering, Saarland*
7 *University, Campus C6.3, 66123 Saarbrücken, Germany*

8 ² *ESRF—The European Synchrotron, CS40220, 38043 Grenoble, France*

9 ³ *Univ Lyon, Université Claude Bernard Lyon 1, CNRS, Institut Lumière Matière, Villeurbanne,*
10 *France*

11 ⁴ *Departament de Física, Universitat Politècnica de Catalunya - BarcelonaTech, ESAB, Esteve*
12 *Terradas 8, 08860 Castelldefels, Spain*

13 ⁵ *Heinz Maier-Leibnitz Zentrum (MLZ) and Physik Department, Technische Universität*
14 *München, Lichtenbergstrasse 1, 85748 Garching, Germany*

15 ⁶ *Dipartimento di Chimica, Università di Pavia, Viale Taramelli 16, 27100 Pavia, Italy*

16

17 *Corresponding author: beatrice.ruta@univ-lyon1.fr

18

19 **Liquid-liquid transitions are interesting to many researchers since they occur in systems**
20 **as diverse as monoatomic liquids, multicomponent oxides and metallic glass-formers. In**
21 **some cases, the crossover is accompanied by changes in the dynamical properties,**
22 **although a direct microscopic evidence of this connection has not been reported so far.**

23 **By combining state-of-the-art synchrotron techniques, we followed the structure and**
24 **atomic motion during quasi-static cooling the Au₄₉Cu_{26.9}Si_{16.3}Ag_{5.5}Pd_{2.3} metallic glass-**
25 **former from the low-temperature supercooled liquid. With this thermal protocol, we were**
26 **able to lower the glass transition temperature far enough to reveal a liquid-liquid**
27 **crossover between two amorphous structures corresponding to two ultra-viscous liquids**
28 **with different kinetic behavior. This transition is in competition with vitrification, which**
29 **occurs at conventional cooling rates, and is accompanied by structural changes not**
30 **affecting the average density. Our results provide a direct connection between**
31 **polyamorphism and dynamical crossover, and an alternative case to add in the highly-**
32 **debated topic on the low-temperature divergence of the dynamics in supercooled liquids.**

33

34 Many systems, ranging from monoatomic liquids [1–3] to amorphous alloys [4–7], exhibit
35 transitions between liquid phases of different local structure. In glass-formers, liquid-liquid
36 transitions (LLTs) have been reported either in high temperature melts [3,8–13] or in
37 supercooled liquids [4–6,14,15], suggesting the existence of intrinsic connections between the
38 kinetic properties of the system and the transition temperature [16]. LLTs are sometime
39 associated to a dynamical crossover with changes in the kinetic fragility [6,10,17]. When
40 observed upon cooling, the liquid evolves from a high temperature fragile phase with a steep
41 temperature dependence of viscosity and structural relaxation time, to a strong phase less
42 affected by temperature changes. For fragile liquids, like molecular and some metallic glass-
43 formers, the LLT is expected at such a low temperature that the system may arrest beforehand
44 in the glass [16]. Still, no direct microscopic evidence of this and more in general of a direct
45 connection between LLT and dynamical crossover have been reported so far. This is also due
46 to the extreme difficulty of obtaining experimental measurements of the atomic collective
47 motion in glass-formers.

48 By taking advantage of state-of-the-art synchrotron techniques like x-ray photon correlation
49 spectroscopy (XPCS) and high energy x-ray diffraction (XRD), we present the first
50 experimental measurements of the microscopic dynamics of an ultra-viscous glass former with
51 relaxation times which were not accessible until now, neither experimentally nor with
52 numerical simulations. Our data show the occurrence of a LLT upon quasi-static cooling the
53 $\text{Au}_{49}\text{Cu}_{26.9}\text{Si}_{16.3}\text{Ag}_{5.5}\text{Pd}_{2.3}$ metallic glass-former, which can be *directly connected* with a fragile-
54 to-strong dynamical crossover. Our thermal approach consists of isothermal steps of 0.5 K at a
55 cooling rate of 0.1 K min^{-1} in the supercooled region between 396 K and 380 K (see SM). With
56 this protocol the glass transition temperature, T_g , is lowered more than 30 degrees in comparison
57 to a standard cooling rate of 20 K min^{-1} , allowing us to unveil the polyamorphic crossover in
58 the ultra-viscous regime as predicted also by Ref. [16]. Interestingly, while the kinetic
59 transition seems to occur at a determined temperature and leads to stationary microscopic
60 dynamics, the structure exhibits much slower transformation rates over a broader transition
61 region. This scenario provides a unique picture of polyamorphism at the atomic level and
62 supports the idea of the formation of a new liquid phase that is locally more ordered and which
63 does not affect the average density, as suggested for other types of complex systems [18–22].

64
65 XPCS experiments were performed at beamline ID10 at ESRF, France. Details on the sample
66 and the technique are reported in the SM. Fig. 1 shows a selection of XPCS data measured at a
67 wave vector $Q_p=2.78 \text{ \AA}^{-1}$ corresponding to the maximum of the structure factor, $S(Q)$, for

68 different isothermal steps between 392 K and 380 K during cooling from the supercooled liquid.
69 These temperatures lie slightly above the T_g for the applied cooling rate, which is determined
70 to be 380 K, thus 33 K below the standard calorimetric $T_g^{\text{end}} = 413$ K (see ref. [23] and SM).
71 The time average intensity auto-correlation functions are reported in Fig. 1a together with the
72 fits with a Kohlrausch-Williams-Watts (KWW) model function: $g_2(Q, t) = 1 + c[\exp(-2(t/\tau)^\beta)]$. Here, τ is the structural relaxation time, β the shape parameter, and c the product between
73 the experimental contrast and the nonergodicity level of the glass, which is basically unity at
74 Q_p [24]. All data are normalized by c , which is found constant at 4%. As discussed in ref. [25],
75 $g_2(Q, t)$ is connected to the decay of density fluctuations and provides information on the
76 collective dynamics at the probed length scale and time interval.
77
78 The quintessential behavior of supercooled liquid dynamics is seen in Fig. 1a. (1) Longer time
79 decays are observed upon cooling, with a dramatic shift of two orders of magnitude from $\sim 10^2$
80 to $\sim 10^4$ s in a span of just 12 K. (2) The shape of the curve is described by a stretched parameter
81 (i.e. $\beta < 1$) with average value of 0.87 ± 0.10 , which is the signature of the heterogeneous
82 dynamics usually found in metallic glass-formers [26–28]. (3) All data collapse onto a single
83 curve when rescaled in reduced time units t/τ confirming the validity of time-temperature
84 superposition (inset Fig. 1a) [29–31].
85
86 The stretched shape of the correlation functions in the supercooled liquid contrasts dramatically
87 with the behavior observed in glasses. At the atomic level, metallic glasses exhibit stress-
88 dominated dynamics characterized by an anomalous compressed decay of the correlation
89 functions (i.e. with $\beta > 1$) [27,32–35], reminiscent of that reported in some soft glasses [25,26]
90 and likely related to microscopic elastic frustrations [36–38]. This is also the case for the system
91 studied in this work. As an example, Fig. 1b shows two normalized $g_2(Q_p, t)$ rescaled in reduced
92 time units, measured both at 383 K but in two different amorphous states reached by following
93 different thermal paths. Open diamonds correspond to a supercooled liquid obtained by
94 applying the quasi-static cooling reported in this work, while the open circles are measured
95 directly at 383 K in a glass produced by melt spinning (i.e. cooled with $\sim 10^6$ K/s). In the glass,
96 the data decay fast and can be modeled with a compressed shape parameter β *two times larger*
97 than the value found in the viscous liquid. Similar stretched behavior of the liquid and
98 compressed behavior of the glass in terms of the $g_2(Q_p, t)$ have been reported also in a Mg-based
99 metallic glass during cooling from the liquid into the glass and vice-versa [33,39]. It is
100 important to note, that even if the data in Fig. 1b are measured at the same temperature, they
101 correspond to dynamics that differ by a factor 15 in time, as schematically shown in the inset,
with τ of ~ 200 s in the glass and of ~ 3000 s in the corresponding ultra-viscous liquid.

102 In the supercooled liquid, the system displays equilibrium dynamics. Representative data are
103 shown in Fig. 1c at 386 K through the evolution of the two-times correlation function (TTCF),
104 which describes the instantaneous correlation between intensity fluctuations in subsequent
105 speckle patterns [25] (see SM). Here, the width of the intensity along the main diagonal is
106 proportional to τ . The atomic dynamics appears stationary with no sign of aging over the entire
107 observation time of 9000 s, thus for a temporal interval ≈ 8 times larger than the corresponding
108 structural relaxation time. This applies to all temperatures but 380 K, the corresponding TTCF
109 is reported in Fig. 2. In this case, we cooled the material from 385.5 K with a rate of 7 K min⁻¹
110 to 380 K without any step. The system is not able to equilibrate during cooling and temporarily
111 freezes into the glass from which it equilibrates in about 2800 s, as indicated by the continuous
112 broadening of the intensity at the beginning of the measurement. After reaching equilibrium,
113 the dynamics is stationary again and the system is in the liquid state, evidenced by a β of
114 0.71 ± 0.05 . The corresponding $g_2(Q_p, t)$ at 380 K is shown in Fig. 1a. It should be noted that
115 equilibration of the ultra-viscous liquid is highly promoted by down-jumps in temperature. This
116 is the reason why the system does not vitrify and remains a supercooled liquid during the whole
117 quasi-static cooling. Differently, the equilibration from the as-quenched glass toward the liquid
118 phase requires much longer times than those probed here. As a consequence, the $g_2(Q_p, t)$
119 measured by heating the glass and shown in Fig. 1b remain compressed with fast relaxation
120 times and no signs of equilibration (i.e. a transition from compressed to stretched and an
121 increase in τ). Asymmetric equilibration mechanisms are typical of glass-formers [40]. They
122 have been also reported in previous XPCS studies [27] and suggest the existence of a strong
123 microscopic barrier to overcome for the equilibration from the glass toward the liquid phase.

124

125 The temperature dependence of the mean relaxation time $\langle \tau \rangle = \Gamma \left(\frac{1}{\beta} \right) \frac{\tau}{\beta}$ obtained from the XPCS
126 data is shown in Fig. 3a. A clear change in the trend is observed at 389 K where $\langle \tau \rangle$ evolves
127 from a steep to a weaker temperature dependence as highlighted in the inset. At a first sight,
128 one would intuitively associate this behavior with the glass transition. This interpretation is,
129 however, *in contradiction* with several observations. (1) The change occurs at a temperature
130 ≈ 10 K above the expected T_g . (2) The shape of the corresponding $g_2(Q_p, t)$ remains stretched
131 without any signature of the stress-dominated dynamics universal for metallic glasses and
132 reported in Fig. 1b for the studied alloy. (3) Evidence of an aging glass is observed only at the
133 lowest investigated temperature of 380 K (Fig. 2), while at higher temperatures the TTCFs
134 exhibit exclusively stationary dynamics of the liquid (Fig. 1c). (4) The relaxation time still

135 displays a pronounced temperature dependence even at low temperatures, which is weaker than
136 that at higher temperatures.

137 To better understand the dynamical results, we employed XRD to investigate the associated
138 structural changes occurring in the material while applying the *identical* thermal protocol. We
139 find a transition from one liquid structure to a different one before the system freezes into a
140 *glass*, which is different from that obtained by faster cooling. This reveals the existence of a
141 complex dynamical pattern that cannot be associated to a simple glass transition.

142 The XRD results are shown in Fig. 3b where we report the temperature dependence of the
143 position of the first sharp diffraction peak (FSDP) of the static structure factor as
144 $(Q_p(T_{\text{ref}})/Q_p(T))^3$, with $T_{\text{ref}}=395.5$ K (see SM). During a standard vitrification, this quantity
145 continuously decreases upon cooling and then bends over to a weaker temperature dependence
146 at T_g , due to the kinetic arrest and the transition into one isoconfiguration of the glass. This is
147 indeed the case for a second dataset, which has been taken by *continuously cooling* the liquid
148 with a *faster rate* of 1.5 K min^{-1} (green open triangles, $T_g=390$ K). XRD data of the quasi-static
149 cooling were collected at the beamline ID11 at ESRF, while the fast-cooled glass was measured
150 at the beamline P02.1 at DESY, Hamburg, Germany (see SM).

151 By applying the quasi-static cooling, T_g is lowered to 380 K. Normally, one would simply
152 expect to observe the same departure from the liquid at this lower temperature (dashed grey line
153 in the figure). In stark contrast to this, $(Q_p(T_{\text{ref}})/Q_p(T))^3$ (blue diamonds) displays a steady
154 anomalous increase between 395.5 and 385.5 K, thus above the expected T_g (see also SM). This
155 increase indicates the occurrence of *pronounced structural changes* in the material which
156 *cannot* be associated to the vitrification. The bend of the XRD data below 380 K also confirms
157 that the glass transition temperature of the strong liquid corresponds to $T_g=380$ K. Additional
158 data taken below this temperature decrease upon cooling with a slope similar to that of the fast-
159 cooled glass (green open triangles). The observed structural changes imply the existence of
160 *different liquid phases* and strongly resemble what has been reported during a LLT in a Zr-
161 based metallic liquid far above T_g [6].

162 In the light of these observations, the dynamical crossover measured by XPCS and shown in
163 Fig. 3a must be associated with the structural changes during the LLT. The data above and
164 below 389 K can be fitted separately with a Vogel-Tamman-Fulcher (VFT) equation $\langle \tau \rangle = \tau_0 \cdot$
165 $\exp\left(\frac{D^* T_0}{T - T_0}\right)$, where τ_0 is the high temperature relaxation time (10^{-14} s), D^* is the kinetic fragility
166 and T_0 is the temperature, at which τ would diverge within this empirical description. The high-
167 temperature liquid exhibits a fragile behavior with $D^* = 8.9 \pm 0.4$ and $T_0 = 315.9 \pm 2.3$ K. This
168 fit is in good agreement with the fragility obtained at higher temperatures from α -relaxation

169 times (open triangles in Fig. 3a) measured using a dynamic mechanical analyzer (DMA, see
170 SM). Differently, the low-temperature liquid is best fitted with $D^* = 23.1 \pm 0.8$ and $T_0 = 243.3$
171 ± 3 K, showing a clearly stronger kinetic nature of that liquid and, hence, a fragile-to-strong
172 LLT in the ultra-viscous state. Similar results can be obtained also by using an Arrhenius model
173 for the data (see SM). The value of D^* obtained for the strong liquid is comparable to that of
174 other strong metallic glass-formers [41,42] in the vicinity of T_g , whereas that obtained for the
175 fragile liquid is among the smallest reported in literature [42,43]. In Zr-based metallic glass-
176 forming systems, for example, such a fragile behavior is typically detected in the stable liquid
177 well above the LLT [4,6,7].

178 Interestingly, the structure of the fragile high-temperature liquid evolves steadily towards the
179 strong low-temperature liquid within a narrow temperature interval of 10 K, whereas the
180 dynamical crossover occurs at a more defined temperature within our resolution. Similar results
181 have been observed in glasses where sudden dynamical changes are accompanied by smeared-
182 out structural modifications [33]. In our case, calorimetric studies show that the associated
183 entropy change during the LLT is very small, i.e. $0.2 \text{ J g-atom}^{-1} \text{ K}^{-1}$, which is in the order of
184 only 2.4% of the entropy of fusion of this system [44]. This suggests the occurrence of
185 extremely slow ordering kinetics during the LLT, as in other systems [22], which cannot be
186 directly associated to a two state crossover scenario [45].

187 As discussed before, the polyamorphic transition is not observed when the system is cooled
188 with a faster rate. In this case, T_g is close to the temperature of the dynamical transition
189 (triangles in Fig. 3b), and the fragile liquid freezes into the glass before the LLT can occur.
190 Between the two competing processes, vitrification is the dominant one. This is obvious if we
191 consider that the glass transition is manifested by marked changes to dynamical quantities,
192 while the structure of a glass is virtually indistinguishable from that of the corresponding
193 supercooled liquid (isoconfigurational) at the moment of freezing. Without major structural
194 modifications, it is therefore clear that vitrification occurs on a much faster time scale than the
195 order-driven LLT, which instead consists of time-consuming structural rearrangements in the
196 highly viscous supercooled liquid state probed here.

197 It is important to stress that the XRD data do not allow to speculate on the evolution of the
198 density during the LLT, as the correlation between the macroscopic density and $1/Q^3$ is not
199 straightforward for multicomponent liquids [13]. This information would require additional
200 macroscopic measurements. In Zr-based metallic glass-formers for instance, the evolution
201 between two liquid phases is accompanied by tiny structural changes (as those reported here)
202 but without any anomaly in the density [6,7]. In that case, thus, the LLT is driven more by

203 changes in the entropy and in the local (chemical) order than by density changes. This could be
204 the case also in our system.

205 We can get some indication on the density from the XPCS data as a change in density would
206 reflect in a change in the decay of the density fluctuations and thus in the temporal evolution of
207 the $g_2(t)$. The stationary dynamics in the XPCS data at each isotherm implies that the density
208 changes only with temperature, although without further information. Differently, it remains
209 constant during the isotherms. This is in agreement with the constant value of $(Q_p(T_{\text{ref}})/Q_p(T))^3$
210 during the isotherms (Fig. 4a and SM) and with the dynamic-to-structure connection recently
211 proposed by some of us [46]. In contrast, the relative change of the FWHM, $\Gamma/\Gamma_0(T_{\text{ref}})$, of the
212 FSDP exhibits a small, but still significant increase with time in the transition region below 391
213 K, whereas there is no evidence of changes above (Fig. 4b, inset and SM). This behavior,
214 together with the stationary dynamics observed with XPCS, suggests the existence of local
215 rearrangements which do not affect the average density. At 380 K, instead, both parameters in
216 Fig. 4 decrease with time as a consequence of the aging towards the equilibrium [46]. As shown
217 in Fig. 2, at this low temperature, the system freezes into the glass upon cooling and
218 subsequently equilibrates within ~ 2800 s. The same applies for the structural metrics in Fig. 4
219 (see also SM) and can be attributed to a densification and medium range ordering during
220 aging [35,46].

221

222 In conclusion, our study reports microscopic evidence of the direct connection between
223 polymorphism and fragile-to-strong dynamical crossover in an ultra-viscous metallic glass-
224 former. In the specific system studied in this work, this phenomenology is usually hidden by
225 the vitrification at higher cooling rates and appears associated with the slow formation of a
226 distinct local order without affecting the average density [18,21]. This scenario shares
227 similarities with the liquid-liquid transitions reported at high temperatures in the Zr- based
228 alloys Vit1 and Vit106a [6,7], and with the case of supercooled Triphenyl Phosphite Ref. [47].
229 In these cases, the transitions are also accompanied by structural changes not affecting the
230 density, without however a direct connection to a fragile-to-strong dynamical crossover. Further
231 studies will clarify whether similar LLTs could occur also in other fragile glass-formers as it
232 was suggested [16] or even in more systems.

233 Finally, it is worth to briefly discuss our results at the light of the current discussions about a
234 possible divergence [48] or not [49–51] of the relaxation time below the conventional glass
235 transition. Our present findings show a specific case where a sudden change in the temperature
236 dependence of the relaxation time in the ultra-viscous regime comes from subtle structural

237 changes in the liquid and not from a dynamical divergence, which could however still occur at
238 lower temperatures.

239

240 **Acknowledgements.** We gratefully thank the ESRF and DESY for providing beamtime. H.
241 Vitoux, K. L’Hoste and F. Zontone are acknowledged for the support during the XPCS
242 measurements at ESRF, Y. Chushkin for providing the code for the analysis of the XPCS data,
243 and J. Bednarcik for the support during the XRD measurements at DESY. We gratefully thank
244 H. Tanaka, W. Hembree and V.M. Giordano for useful discussions. I. Gallino acknowledges
245 financial support from the DFG Grant No. GA 1721/2-2. E. Pineda acknowledges financial
246 support from MINECO, grant FIS2014-54734-P, and Generalitat de Catalunya, grant
247 2014SGR00581.

248

249

250

251 **References**

252 [1] P. F. McMillan, M. Wilson, D. Daisenberger, and D. Machon, *Nat. Mater.* **4**, 680
253 (2005).

254 [2] S. Sastry and C. Austen Angell, *Nat. Mater.* **2**, 739 (2003).

255 [3] M. H. Bhat, V. Molinero, E. Soignard, V. C. Solomon, S. Sastry, J. L. Yarger, and C.
256 A. Angell, *Nature* **448**, 787 (2007).

257 [4] C. Way, P. Wadhwa, and R. Busch, *Acta Mater.* **55**, 2977 (2007).

258 [5] Z. Evenson, T. Schmitt, M. Nicola, I. Gallino, and R. Busch, *Acta Mater.* **60**, 4712
259 (2012).

260 [6] S. Wei, F. Yang, J. Bednarcik, I. Kaban, O. Shuleshova, A. Meyer, and R. Busch, *Nat.*
261 *Commun.* **4**, 2083 (2013).

262 [7] M. Stolpe, I. Jonas, S. Wei, Z. Evenson, W. Hembree, F. Yang, A. Meyer, and R.
263 Busch, *Phys. Rev. B* **93**, 14201 (2016).

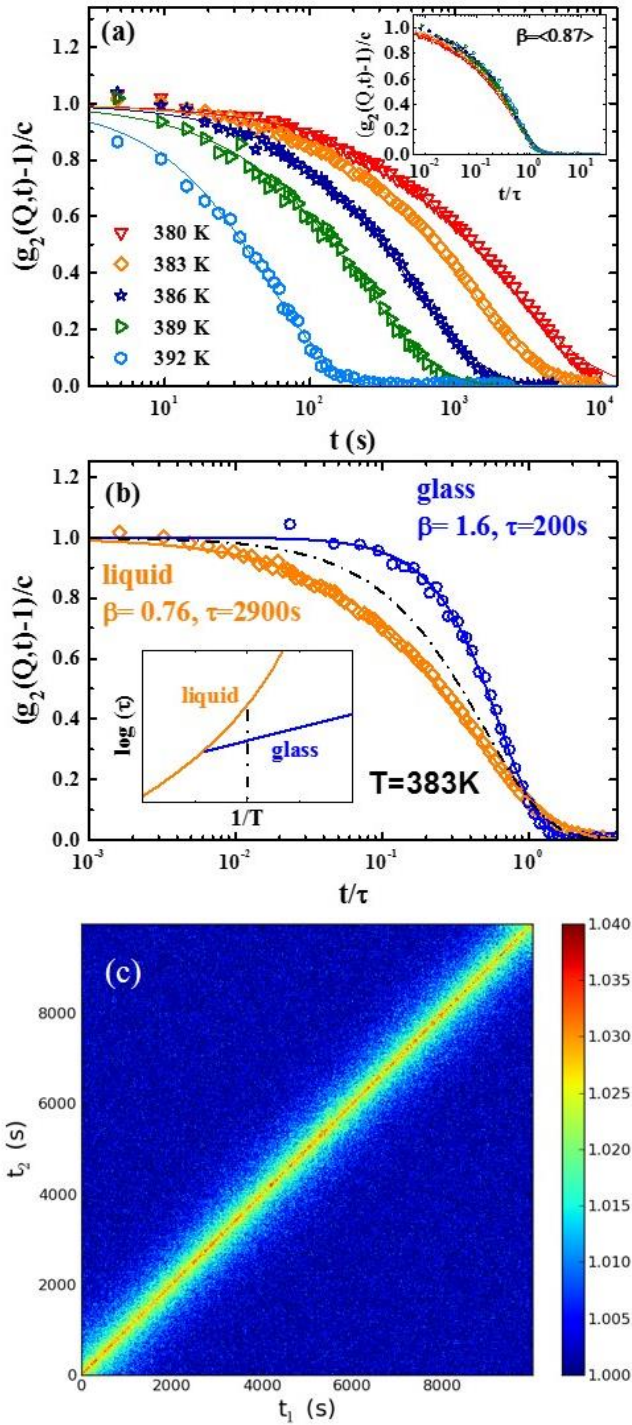
264 [8] S. Aasland and P. F. McMillan, *Lett. to Nat.* **369**, 633 (1994).

265 [9] Y. Katayama, T. Mizutani, W. Utsumi, O. Shimomura, M. Yamakata, and K.

- 266 Funakoshi, Nature **403**, 170 (2000).
- 267 [10] I. Saika-Voivod, P. H. Poole, and F. Sciortino, Nature **412**, 514 (2001).
- 268 [11] V. Molinero, S. Sastry, and C. A. Angell, Phys. Rev. Lett. **97**, 75701 (2006).
- 269 [12] A. Jaiswal, A. Podlesynak, G. Ehlers, R. Mills, S. O’Keeffe, J. Stevick, J. Kempton, G.
270 Jelbert, W. Dmowski, K. Lokshin, T. Egami, and Y. Zhang, Phys. Rev. B - Condens.
271 Matter Mater. Phys. **92**, 24202 (2015).
- 272 [13] W. Xu, M. T. Sandor, Y. Yu, H.-B. Ke, H.-P. Zhang, M.-Z. Li, W. H. Wang, L. Liu,
273 and Y. Wu, Nat. Commun. **6**, 7696 (2015).
- 274 [14] P. Gallo, K. Amann-Winkel, C. A. Angell, M. A. Anisimov, F. Caupin, C.
275 Chakravarty, E. Lascaris, T. Loerting, A. Z. Panagiotopoulos, J. Russo, J. A. Sellberg,
276 H. E. Stanley, H. Tanaka, C. Vega, L. Xu, and L. G. M. Pettersson, Chem. Rev. **116**,
277 7463 (2016).
- 278 [15] S. Wei, M. Stolpe, O. Gross, W. Hembree, S. Hechler, J. Bednarcik, R. Busch, and P.
279 Lucas, Acta Mater. **129**, 259 (2017).
- 280 [16] C. A. Angell, MRS Bull. **33**, 544 (2011).
- 281 [17] A. Faraone, L. Liu, C.-Y. Mou, C.-W. Yen, and S. H. Chen, J. Chem. Phys. **121**, 10843
282 (2004).
- 283 [18] H. Tanaka, Phys. Rev. E **62**, 6968 (2000).
- 284 [19] H. Tanaka, R. Kurita, and H. Matakai, Phys. Rev. Lett. **92**, 25701 (2004).
- 285 [20] K. Murata and H. Tanaka, Nat. Mater. **11**, 436 (2012).
- 286 [21] H. Tanaka, Eur. Phys. J. E **35**, 113 (2012).
- 287 [22] M. Kobayashi and H. Tanaka, Nat. Commun. **7**, 13438 (2016).
- 288 [23] Z. Evenson, S. E. Naleway, S. Wei, O. Gross, J. J. Kruzic, I. Gallino, W. Possart, M.
289 Stommel, and R. Busch, Phys. Rev. B **89**, 174204 (2014).
- 290 [24] B. Ruta, G. Monaco, V. M. Giordano, F. Scarponi, D. Fioretto, G. Ruocco, K. S.

- 291 Andrikopoulos, and S. N. Yannopoulos, *J. Phys. Chem. B* **115**, 14052 (2011).
- 292 [25] A. Madsen, A. Fluerasu, and B. Ruta, in *Synchrotron Light Sources Free. Lasers*
293 (Springer International Publishing, Cham, 2015), pp. 1–21.
- 294 [26] L. Cipelletti, L. Ramos, S. Manley, E. Pitard, D. A. Weitz, E. E. Pashkovski, and M.
295 Johansson, *Faraday Discuss.* **123**, 237 (2003).
- 296 [27] B. Ruta, Y. Chushkin, L. Cipelletti, E. Pineda, P. Bruna, and V. M. Giordano, *Phys.*
297 *Rev. Lett.* **109**, 165701 (2012).
- 298 [28] L. Berthier, *Physics (College. Park. Md.)* **4**, 7 (2011).
- 299 [29] D. Richter, B. Frick, and B. Farago, *Phys. Rev. Lett.* **61**, 2465 (1988).
- 300 [30] P. Lunkenheimer, R. Wehn, U. Schneider, and A. Loidl, *Phys. Rev. Lett.* **95**, 55702
301 (2005).
- 302 [31] N. B. Olsen, T. Christensen, and J. C. Dyre, *Phys. Rev. Lett.* **86**, 1271 (2001).
- 303 [32] Z. Evenson, B. Ruta, S. Hechler, M. Stolpe, E. Pineda, I. Gallino, and R. Busch, *Phys.*
304 *Rev. Lett.* **115**, 175701 (2015).
- 305 [33] B. Ruta, V. M. Giordano, L. Erra, C. Liu, and E. Pineda, *J. Alloys Compd.* **615**, 45
306 (2014).
- 307 [34] B. Ruta, G. Baldi, G. Monaco, and Y. Chushkin, *J. Chem. Phys.* **138**, 54508 (2013).
- 308 [35] B. Ruta, E. Pineda, and Z. Evenson, *J. Phys. Condens. Matter* **29**, (2017).
- 309 [36] P. Chaudhuri and L. Berthier, *arXiv* **1605**, 097770v1 (2016).
- 310 [37] E. E. Ferrero, K. Martens, and J. L. Barrat, *Phys. Rev. Lett.* **113**, 248301 (2014).
- 311 [38] M. Bouzid, J. Colombo, L. V. Barbosa, and E. Del Gado, *Nat. Commun.* **8**, 15846
312 (2016).
- 313 [39] B. Ruta, Y. Chushkin, and G. Monaco, *AIP Conf. Proc.* **1518**, 181 (2013).
- 314 [40] C. A. Angell, K. L. Ngai, G. B. McKenna, P. F. McMillan, and S. W. Martin, *J. Appl.*
315 *Phys.* **88**, 3113 (2000).

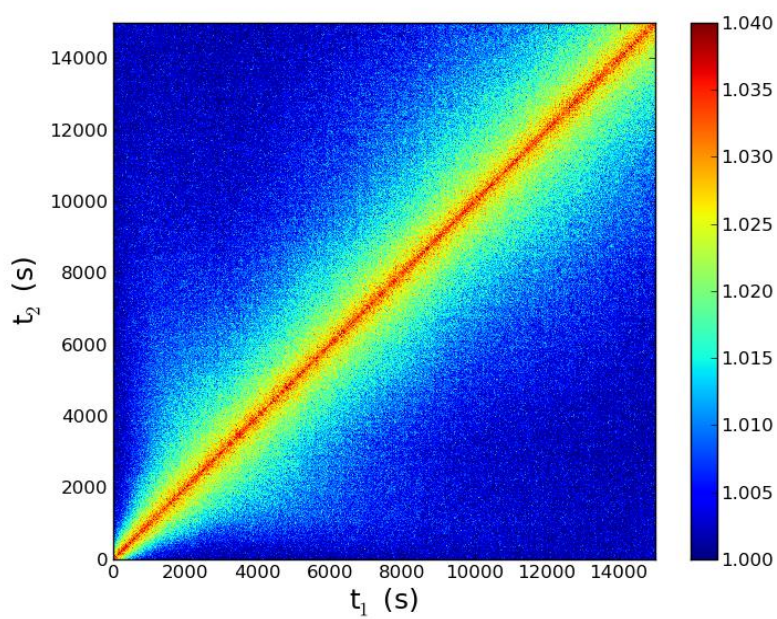
- 316 [41] R. Busch, W. Liu, and W. L. Johnson, *J. Appl. Phys.* **83**, 4134 (1998).
- 317 [42] I. Gallino, J. Schroers, and R. Busch, *J. Appl. Phys.* **108**, 1 (2010).
- 318 [43] O. Gross, B. Bochtler, M. Stolpe, S. Hechler, W. Hembree, R. Busch, and I. Gallino,
319 *Acta Mater.* **132**, 118 (2017).
- 320 [44] I. Gallino, D. Cangialosi, Z. Evenson, L. Schmitt, S. Hechler, and B. Ruta, arXiv **1706**,
321 3830 (2017).
- 322 [45] H. Tanaka, *J. Phys. Condens. Matter* **15**, L703 (2003).
- 323 [46] V. M. Giordano and B. Ruta, *Nat. Commun.* **7**, 10344 (2015).
- 324 [47] M. Kobayashi and H. Tanaka, *Nat. Commun.* **7**, 13438 (2016).
- 325 [48] G. Adam and J. H. Gibbs, *J. Chem. Phys.* **43**, 139 (1965).
- 326 [49] J. Zhao, S. L. Simon, and G. B. Mckenna, *Nat. Commun.* **4**, 1783 (2013).
- 327 [50] E. Arianna, A. Pogna, C. Rodríguez-Tinoco, G. Cerullo, C. Ferrante, and J. Rodríguez-
328 viejo, *PNAS* **112**, 2331 (2015).
- 329 [51] T. Hecksher, A. I. Nielsen, N. B. Olsen, and J. C. Dyre, *Nat. Phys.* **4**, 737 (2008).



330

331 **Figure 1:** (a) Temperature dependence of normalized intensity autocorrelation functions
 332 measured with XPCS at $Q_p=2.78 \text{ \AA}^{-1}$. Lines are fits using the KWW function. **Inset:** Same data
 333 reported as t/τ . (b) $g_2(Q_p,t)-1/c$ as a function of t/τ measured at 383 K in an hyperquenched glass
 334 heated from low temperature (blue circles), and in the supercooled liquid shown in panel (a)
 335 (orange diamonds). The dashed line is a single exponential decay. The two curves correspond
 336 to two distinct dynamics as sketched in the inset by the intersection of the vertical line with the
 337 glass or the liquid. (c) TTCF at 386 K showing stationary dynamics.

338

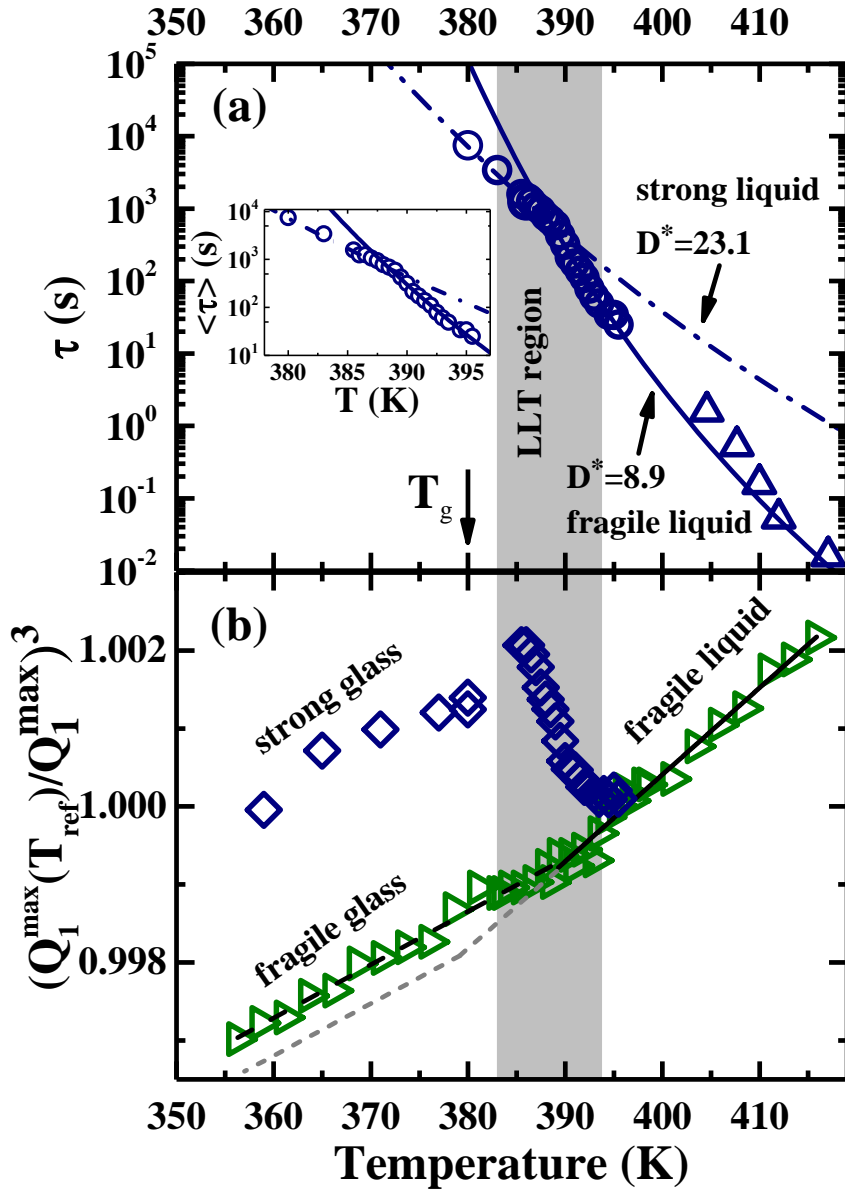


339

340 **Figure 2:** TCF measured with XPCS at 380 K after quenching from 385.5 K with 7 K min⁻¹.
341 The broadening at short times due to equilibration stops after ~2800 s.

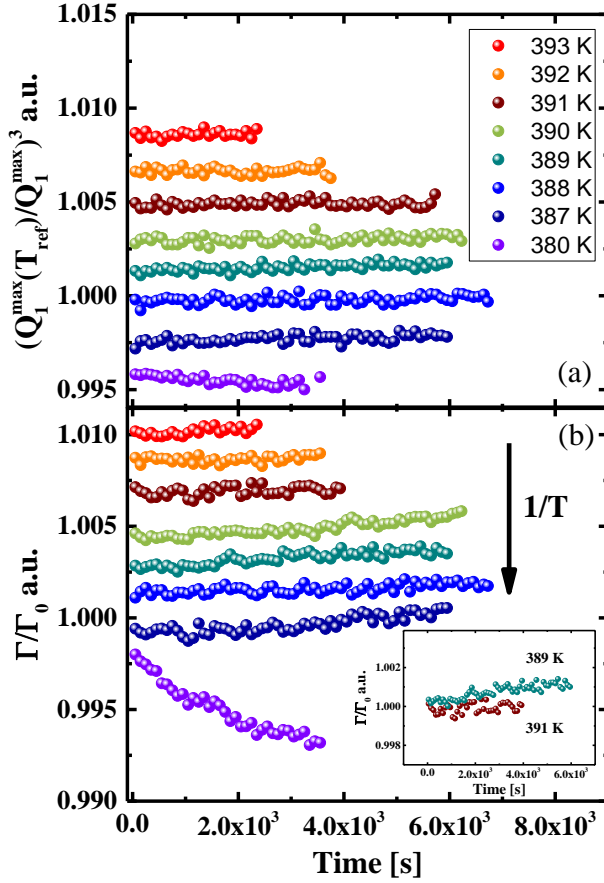
342

343



344

345 **Figure 3:** (a) Temperature dependence of τ measured by XPCS (circles) and DMA (triangles).
 346 The LLT occurs at 389 K leading to two regimes with distinct fragilities (magnified in the inset).
 347 (b) Temperature dependence of the relative shift $(Q_1^{\max}(T_{\text{ref}})/Q_1^{\max})^3$ of the FSDP measured
 348 with XRD by continuous cooling with 1.5 K min^{-1} (green triangles), and by applying the quasi-
 349 static protocol used for the XPCS data (blue diamonds). The grey dashed line shows the
 350 standard behavior that one would have expected to see in absence of the LLT.



351

352 **Figure 4:** Temporal evolution of $(Q_1^{\max}(T_{\text{ref}})/Q_1^{\max})^3$ (a) and FWHM (b) during isotherms at
 353 selected temperatures between 395.5 k and 380 K. All data are vertically shifted for clarity. We
 354 can distinguish three different behaviors: 1) at high temperature between 395.5 k and 391 K,
 355 both $(Q_1^{\max}(T_{\text{ref}})/Q_1^{\max})^3$ and the FWHM are constant with time; 2) between 390 and 385.5 K
 356 $(Q_1^{\max}(T_{\text{ref}})/Q_1^{\max})^3$ remains constant while the FWHM slightly increases with time. This
 357 behavior can be attributed to changes in the local order not affecting the average density; 3) At
 358 the glass transition temperature of the quasi-static cooling, i.e. 380 K, both parameters decrease
 359 due to aging and thus to the equilibration at short times from the glass toward the liquid phase.
 360 The same equilibration is also observed in the dynamics in Fig. 2.

361